



Published in final edited form as:

Neuropsychopharmacology. 2010 February ; 35(3): 806–817. doi:10.1038/npp.2009.189.

Impact of D2 receptor internalization on binding affinity of neuroimaging radiotracers

Ningning Guo^{1,7}, Wen Guo², Michaela Kralikova², Man Jiang^{1,6}, Ira Schieren³, Raj Narendran^{1,7}, Mark Slifstein^{1,7}, Anissa Abi-Dargham^{1,7}, Marc Laruelle^{1,4,5,*}, Jonathan A. Javitch^{1,2,6,*}, and Stephen Rayport^{1,6,*}

¹Departments of Psychiatry, Columbia University, New York, NY

²Center for Molecular Recognition, Columbia University, New York, NY

³Howard Hughes Medical Institute, Columbia University, New York, NY

⁴Neurosciences Center for Excellence in Drug Discovery GlaxoSmithKline, London, UK

⁵Department of Neuroscience, Imperial College, London, UK

⁶Molecular Therapeutics, New York State Psychiatric Institute, New York, NY

⁷Translational Imaging, New York State Psychiatric Institute, New York, NY

Abstract

Synaptic dopamine levels appear to affect the *in vivo* binding of many D2 receptor radioligands. Thus, release of endogenous dopamine induced by administration of amphetamine decreases ligand binding, whereas subchronic dopamine depletion increases binding. This is generally thought to be due to binding competition between endogenous dopamine and the radioligands. However, the temporal dissociation between amphetamine-induced increases in dopamine, which last on the order of 2 hours as measured by microdialysis, and the prolonged decrease in ligand binding, which lasts on the order of a day, has suggested that agonist-induced D2 receptor internalization may contribute to the sustained decrease in D2 receptor binding potential seen following a dopamine surge. To test this hypothesis, we developed an *in vitro* system showing robust agonist-induced D2 receptor internalization following treatment with the agonist quinpirole. HEK293 cells were stably co-transfected with human D2 receptor, G-protein-coupled-receptor kinase 2 and arrestin 3. Agonist-induced D2 receptor internalization was demonstrated by fluorescence microscopy, flow cytometry and radioligand competition binding. The binding of seven antagonists and four agonists to surface and internalized receptors was measured in intact cells. All imaging ligands bound with high affinity to both surface and internalized D2 receptors. Affinity to internalized receptors was modestly lower, supporting the hypothesis that

Users may view, print, copy, download and text and data- mine the content in such documents, for the purposes of academic research, subject always to the full Conditions of use: http://www.nature.com/authors/editorial_policies/license.html#terms

*Correspondence: Stephen Rayport (sgr1@columbia.edu), Jonathan A. Javitch (jaj2@columbia.edu) or Marc Laruelle (m.laruelle@imperial.ac.uk)..

CONFLICT OF INTEREST DISCLOSURE

Jonathan A. Javitch is on the Scientific Advisory Board of HEPTARES therapeutics. Marc Laruelle is an employee of GlaxoSmithKline. Stephen Rayport is a Scientific Consultant to MatTek. The other authors have no conflicts of interest to disclose.

Supplementary Information is available at the *Neuropsychopharmacology* website.

internalization would reduce binding potential measured in imaging studies performed with these ligands. However, between-ligand differences in the magnitude of the internalization-associated affinity shift only partly accounted for the data obtained in neuroimaging experiments, suggesting that mechanisms beyond competition and internalization are involved.

Keywords

dopamine; raclopride, sulpiride, imaging; endogenous competition; HEK293 cells

INTRODUCTION

Many studies have shown that acute fluctuations in synaptic dopamine (DA) affect the *in vivo* binding of D₂ receptor radioligands used in Single Photon Emission Computed Tomography (SPECT) and Positron Emission Tomography (PET) studies (for review, see Laruelle, 2000). An increase in DA release, such as that induced by amphetamine administration, leads to an acute decrease in the *in vivo* binding of imaging ligands. Conversely, reducing DA release by DA depletion leads to an increase in the *in vivo* binding of the ligands. The recognition of this phenomenon in animals inspired the methodology to measure changes in synaptic DA in humans with SPECT using IBZM and with PET using raclopride. This methodology has been used extensively to study alterations in DA transmission in schizophrenia (Abi-Dargham *et al*, 2000; Breier *et al*, 1997; Laruelle *et al*, 1996) and substance abuse (Martinez *et al*, 2007; Volkow *et al*, 1997), as well as the effects of stimulants on DA neurotransmission (Kegeles *et al*, 2000; van Berckel *et al*, 2006; Volkow *et al*, 2009).

The ability of neuroimaging ligands to report on changes in synaptic DA has been validated by two key observations. In humans, DA depletion blocks the effect of stimulants on the *in vivo* binding of PET radiotracers (Laruelle *et al*, 1997a). In nonhuman primates, the magnitude of DA release, as measured with microdialysis, correlates with the decrease in D₂ receptor binding potential (BP, the ratio of receptor number to affinity, B_{\max}/K_D), as measured with PET or SPECT (Breier *et al*, 1997; Laruelle *et al*, 1997b). These interactions have been reliably observed with moderate-to-high affinity D₂ receptor benzamide antagonists, [¹¹C]raclopride ($K_D = 1$ nM), [¹²³I]IBZM ($K_D = 0.2$ nM), and [¹⁸F]fallypride ($K_D = 0.2$ nM) (Cropley *et al*, 2008; Laruelle, 2000; Mukherjee *et al*, 2005; Narendran *et al*, 2009; Riccardi *et al*, 2006; Slifstein *et al*, 2004), but inconsistently with the very-high affinity D₂ receptor antagonists [¹¹C]N-methylspiperone ([¹¹C]NMSP, $K_D = 0.07$ nM), [¹¹C]FLB457 ($K_D = 0.03$ nM) and [¹²³I]epidepride ($K_D = 0.01$ nM) (Aalto *et al*, 2009; Laruelle, 2000; Narendran *et al*, 2009). This divergence may be due to physiochemical differences among the ligands, or to technical difficulties encountered in quantification of striatal D₂ receptor availability with very-high affinity ligands. Studies with the radiolabeled D₂ receptor agonists [¹¹C]NPA and [¹¹C]PHNO have demonstrated that the *in vivo* binding of these tracers is also sensitive to changes in synaptic DA (Ginovart *et al*, 2006; Narendran *et al*, 2004; Narendran *et al*, 2006).

While it is generally accepted that competition between D₂ radioligands and endogenous DA affects the binding of the ligands at D₂ receptors, the temporal discrepancy between changes in DA levels and radioligand binding is not fully explained by the competition model. Following intravenous amphetamine administration, the increase in extracellular DA and behavioral activation lasts about 2 hours (Ichikawa and Meltzer, 1992; Laruelle *et al*, 1997b), while the *in vivo* decrease in D₂ receptor BP measured with PET or SPECT ligands lasts about 24 hours (Carson *et al*, 2001; Laruelle *et al*, 1997b; Narendran *et al*, 2007). G-protein coupled receptors (GPCRs), including D₂ receptors, show agonist-induced internalization (Goggi *et al*, 2007; Ito *et al*, 1999; Macey *et al*, 2004; Paspalas *et al*, 2006; Vickery and von Zastrow, 1999), which might account for the temporal discrepancy (Laruelle, 2000).

Like most GPCRs, D₂ receptor internalization is regulated by GPCR kinases (GRKs) and arrestins (Heusler *et al*, 2008; Ito *et al*, 1999; Kim *et al*, 2001; Macey *et al*, 2004; Namkung *et al*, 2009), which target the receptor to clathrin-coated pits for internalization (Perry and Lefkowitz, 2002; Tsao *et al*, 2001). Agonist-induced internalization of D₂ receptors would result in a reduction in BP if the affinity of the ligands for the receptors was reduced by internalization, which might be due to diminished ligand access or to changes in receptor conformation in the microenvironment associated with internalization.

To address the role of D₂ receptor internalization in the readout of neuroimaging ligands, we developed an *in vitro* system to measure binding to surface and internalized D₂ receptors independently. Human embryonic kidney 293 (HEK293) cells were stably transfected with D₂ receptors (Javitch *et al*, 2000) tagged with enhanced yellow-fluorescent protein (EYFP), and co-transfected with GRK2 and arrestin3 to foster robust D₂ receptor internalization. We demonstrate that these cells show robust D₂ receptor internalization, allowing us to address the effect of receptor internalization on the binding of most-used neuroimaging ligands.

MATERIALS AND METHODS

Cell system

T-REx-293 cells, a Tetracycline-Regulated Expression cell line (Invitrogen, Carlsbad, CA) were grown in Dulbecco's modified Eagle's medium (GIBCO) containing 10% fetal calf serum and 5 µg/ml blasticidin at 37 °C with 5% CO₂, and passaged weekly. The bovine GRK2 and rat arrestin3 cDNAs were subcloned into T-REx expression plasmids pcDNA4/TO and pcDNA5/TO (Invitrogen), respectively, and confirmed by sequencing. The human short isoform of D₂ receptor (D2S) cDNA with a signal peptide and FLAG epitope at the amino terminus was fused with EYFP at the carboxyl terminus and subcloned into the bicistronic expression vector pCIN4 (Javitch *et al*, 2000; Rees *et al*, 1996). The constructs pcDNA4-GRK2 and pcDNA5-arrestin3 were serially cotransfected into the T-REx-293 cells using lipofectamine (Invitrogen). Zeocin- and hygromycin-resistant cells were selected. GRK2 and arrestin3 expression were examined by immunoblotting following tetracycline induction (see below). Construct pCIN4-D2S was then transfected into the stable doubly transfected cells, and the triple-transfected cells were selected in the presence of 700 µg/ml G418, in addition to hygromycin, Zeocin and blasticidin.

Western blot analysis

Control T-REx-293 and the triple-transfected cells were treated with tetracycline or vehicle for 24 h, and then solubilized with 1% dodecyl maltopyranoside in PBS buffer (11 mM Na₂HPO₄, 154 mM NaCl, 2.7 mM KCl, 1 mM MgCl₂, 0.1 mM CaCl₂, 2 µg/ml pefabloc, 2 µg/ml aprotinin, 1 µg/ml leupeptin, 1 µg/ml pepstatin A, and 10 mM N-ethylmaleimide). 20 µg of protein lysates were separated by SDS-PAGE using a 7.5% polyacrylamide gel and transferred to a polyvinylidene difluoride (PVDF) membrane (Millipore, Bedford, MA). Membranes were blocked for 30 min at room temperature with 5% nonfat milk, 1% bovine serum albumin, 0.1% Tween 20 in Tris-buffered saline (TBST; 50 mM Tris-HCl, 150 mM NaCl, pH 7.4). Primary antibodies, anti-GRK2 rabbit polyclonal (1:1000, Santa Cruz Biotechnology), anti-arrestin3 rabbit polyclonal (1:500, Sigma-Aldrich), and anti-FLAG rabbit polyclonal (1:10,000, Sigma-Aldrich) were incubated with the PVDF membranes at room temperature for 1 h to detect GRK2, arrestin3 and D₂ receptor, respectively. Membranes were then washed three times for 10 min each with TBST, incubated with horseradish peroxidase-conjugated anti-rabbit-antibody (1:15,000, Santa Cruz Biotechnology) at room temperature for 1 h, and washed three times. Immunoblots were treated with ECL-Plus reagent (Amersham Biosciences, Piscataway, NJ); proteins were visualized and quantitated on a FluorChem 8000 (Alpha Innotech Corporation, San Leandro, CA).

Drug treatment

Tetracycline—Triple-transfected cells were grown in 100 mm culture dishes for 3-5 days until they were 80-90% confluent. To induce expression of GRK2 and arrestin3, tetracycline was added to the cells (T+) at a final concentration of 1 µg/ml for 24 h at 36 °C. Control cells (T-) were incubated with the same volume of vehicle solution.

Quinpirole—To induce D₂ receptor internalization, tetracycline-treated (T+) and control (T-) cells were incubated with quinpirole (T+/Q+; T-/Q+) at a final concentration of 30 µM for 3 h at 36 °C. Control cells (T+/Q-, T-/Q-) were incubated with vehicle. After quinpirole treatment, the medium was removed and the cells were washed with 10 ml PBS (pH 7.4) at 4 °C and used in the immuno-labeling or radioligand binding procedures as described. Since neither tetracycline alone nor basal expression of GRK2 and arrestin3 affected D₂R internalization, all radioligand binding studies were performed on tetracycline treated cells.

MTSET—The sulfhydryl-specific reagent [2-(trimethylammonium)ethyl] methanethiosulfonate bromide (MTSET) is a membrane-impermeant, positively charged polar molecule that reacts with the sulfhydryl group of Cys114 in the binding site crevice of the D₂ receptor to inhibit ligand binding (Javitch *et al.*, 1994; Javitch *et al.*, 2000). MTSET was used to inactivate cell surface D₂ receptors selectively. Aliquots of control and quinpirole-treated cell suspensions (100 µl) were incubated with freshly dissolved MTSET at final concentrations of 0.03 mM to 10 mM at 4 °C for 15 min. In competition and saturation binding studies, cells were incubated with 5 mM MTSET. The reaction was slowed by addition of cold binding buffer to the cell suspensions to a final volume of 500 µl (see below).

Immunohistochemistry and flow cytometry quantification

To visualize internalization, cells were washed three times with ice-cold HEPES saline buffer (25 mM HEPES, 140 mM NaCl, 5.4 mM KCl, 10% goat serum, pH 7.4). An anti-FLAG labeling mixture was prepared by adding 5 μg Zenon-Alexa 647 mouse IgG labeling reagent A (Invitrogen) to 0.4 μg anti-FLAG antibody in 15 μl PBS (without Ca^{2+} and Mg^{2+}) at room temperature for 5 min then adding 5 μg IgG labeling reagent B and incubating for 5 minutes, adjusting the total volume to 100 μl by adding 10% goat serum in HEPES buffered saline. For fluorescence microscopic imaging, we applied the labeling mixture to cells grown in microwell dishes (MatTek, Ashland, MA) and incubated for 40 min at 4 $^{\circ}\text{C}$. Cells were washed with HEPES buffered saline three times, and viewed using an Axiovert 35M (Zeiss). Digital images were captured (Photometrics Sensys camera, Roper Scientific, Tucson, AZ) with iVision software (BioVision, Exton, PA). Sequential imaging was done using a diamond objective scribe to mark regions of interest. Zenon-fluorescence labeling identified surface D_2 receptors, and EYFP labeling both surface and internalized receptors.

For flow cytometry, dissociated cells were incubated under the same conditions. Surface receptors were labeled via the transfected D_2 receptor N-terminal FLAG-tag with anti-FLAG-mouse and anti-mouse-PE antibodies (Invitrogen) diluted 1:500 in phosphate buffered saline (with 0.1% of BSA and 0.1% of NaN_3), and quantitated using a Guava EasyCyte (Millipore).

Radioligand binding

Whole cell suspension—Cells were dissociated by gentle trituration in 3 ml of binding buffer (25 mM HEPES, 140 mM NaCl, 5.4 mM KCl, 0.006% BSA, 1 mM EDTA, pH 7.4) at 4 $^{\circ}\text{C}$, counted with a hemocytometer, and diluted with cold binding buffer to make the cell suspension of $1.9 \times 10^6 - 2.8 \times 10^6$ cells/ml. To reduce oxidation of DA and D_2 agonists in competition binding assays, 0.1% ascorbic acid was added to the binding buffer.

Competition binding—To determine whether [^3H]N-methylspiperone (NMSP) and [^3H]raclopride bound to both surface and internalized D_2 receptors, sulpiride, a D_2 antagonist with a fixed negative charge, was used as a competitor at surface receptors. Intact cells (100 μl of cell suspension) were incubated with 100 μl of sulpiride at final concentrations of $10^{-13} - 10^{-3}$ M and 100 μl of radioligand [^3H]NMSP (0.3 ± 0.1 nM) or [^3H]raclopride (1.5 ± 0.5 nM), respectively. A minimum of 6 independent experiments was carried out for each of the imaging agents (raclopride, IBZM, NMSP, fallypride, FLB 457, epidepride, PHNO and NPA) and control agents (quinpirole, dopamine and sulpiride). Nonspecific binding was determined in the presence of 10 μM (+)-butaclamol. Each binding experiment was performed in duplicate, and the reaction mixtures (final volume 500 μl) were vortexed and then incubated at 4 $^{\circ}\text{C}$ for 3.5 hrs. The incubation was terminated by rapid filtration on a Cell Harvester (Brandel, Gaithersburg, MD) through GF/B filters pretreated with 0.3% polyethyleneimine. The filters were washed four times with ice-cold Tris-HCl buffer (10 mM Tris-HCl, 120 mM NaCl, pH 7.4), and the radioactivity on the filters was counted with a scintillation counter (Packard, Meriden, CT). The competition curves were analyzed by comparison of two-site vs. one-site binding models with nonlinear curve-fitting (Prism 4, GraphPad Software, San Diego, CA).

Saturation binding—Following MTSET treatment, which blocks binding of ligands to surface D₂ receptors, cells (100 μ l) were incubated with six concentrations of [³H]NMSP (0.008 – 0.6 nM) or [³H]raclopride (0.25 – 6.0 nM) in a final volume of 500 μ l. Specific binding was defined as the total binding minus the nonspecific binding obtained in the presence of 10 μ M (+)-butaclamol. The binding was performed in duplicate at 4 °C for 3.5 hrs and terminated by rapid filtration on the Cell Harvester. The K_D and B_{max} values were determined by curve-fitting (Prism 4).

RESULTS

Tetracycline induced GRK2 and arrestin3 expression

T-REx-293 cells stably expressing D₂-EYFP receptors were engineered to allow tetracycline-induced expression of GRK2 and arrestin3 to facilitate robust agonist-induced D₂ receptor internalization. Both control T-REx-293 and triple-transfected cells showed low basal expression of GRK2 and arrestin3 (Figure 1a). Tetracycline increased GRK2 and arrestin3 expression dramatically, with 190 \pm 24 % increases in GRK2 (n=3) and 538 \pm 75 % in arrestin3 (n=2) expression in the triple-transfected cells, compared to untreated cells.

Visualization of D₂ receptor internalization

Monolayers of triple-transfected cells were examined when they were close to confluence (Figure 1B1). The enhancement of GRK2 and arrestin3 expression resulted in robust agonist-induced D₂ receptor internalization. Under control conditions (without tetracycline or quinpirole, T-/Q-, or tetracycline alone, T+/Q-), D₂ receptors were mainly expressed on the cell surface, as indicated by the surface fluorescence of EYFP tagged D₂ receptors (Q-, Figure 1B2). Following tetracycline induction and quinpirole treatment (T+/Q+), EYFP labeled receptors shifted to the cytoplasm, forming a characteristic punctate endocytic distribution (Q+, Figure 1B3). Since neither tetracycline nor quinpirole alone induced D₂ receptor internalization, cells were pretreated with tetracycline in all subsequent imaging and binding experiments, and internalization was induced by quinpirole treatment.

Quantitation of internalization with flow cytometry

To detect internalization, we used Zenon labeled anti-FLAG F_{ab} fragments directed to the FLAG epitope on the extracellular N-terminus of the D₂ receptors. Under control conditions, nearly all D₂ receptors were located on the surface, as the EYFP fluorescence (visualized in red) and Zenon fluorescence (visualized in green) overlapped (appearing yellow), outlining the plasma membrane (Figure 2a1). Following quinpirole treatment, surface labeling diminished (less yellow), and many receptors internalized, appearing in a punctate intracellular pattern (red) (Figure 2a2). We used flow cytometry to quantify internalization by analyzing anti-FLAG labeling of surface receptors (Figure 2b). An example of the distribution of fluorescence intensity for surface D₂ receptors before (black) and after (red) quinpirole administration is shown in Figure 2B1. Time course studies revealed maximal D₂ receptor internalization of about 58% following quinpirole treatment with a t_{1/2} of 5.3 \pm 0.7 min (Figure 2B2).

Internalization quantification with [³H]NMSP and [³H]raclopride binding studies

[³H]NMSP binding—To measure binding to internalized D₂ receptors in intact cells, we treated cells with quinpirole, inactivated the remaining surface receptors with MTSET, and performed binding using the lipophilic ligand [³H]NMSP. Consistent with the fluorescence imaging data, [³H]NMSP binding showed, under baseline conditions, that most D₂ receptors were susceptible to inactivation by membrane-impermeant MTSET, and therefore on the surface. [³H]NMSP binding in control cells (Q⁻) dropped to 10% of the total binding in the presence of MTSET (3-10 mM; Figure 3A), indicating that under control conditions ~90% of receptors were on the cell surface. After quinpirole treatment (Q⁺), MTSET inactivated only about 50% of [³H]NMSP binding (Figure 3A), indicating that about 40% of D₂ receptors underwent internalization, and were thus protected from MTSET inactivation.

Sulpiride competition with [³H]NMSP revealed a two-site binding curve under control conditions (Q⁻), with the majority of D₂ receptors showing a high affinity (89.9%, K_i = 9.1 ± 1.0 nM) and the minority showing a very low affinity (10.1%, K_i = 142.5 ± 26.8 μM, Figure 3B). Because sulpiride is relatively impermeant due to its fixed negative charge (Honda *et al*, 1977; Mizuchi *et al*, 1983), the high affinity sites presumably correspond to surface D₂ receptors (K_{i(s)}) and the low affinity sites to D₂ internalized receptors (K_{i(i)}). Following quinpirole treatment (Q⁺), 55% of D₂ receptors retained high affinity (K_{i(s)} = 9.4 ± 2.6 nM), whereas 45% displayed low affinity (K_{i(i)} = 142.9 ± 26.3 μM), indicating that about 35% of receptors underwent internalization (Figure 3B).

[³H]raclopride binding and raclopride competition—Due to its lower lipophilicity compared to NMSP, we expected that raclopride would have more limited access to internalized D₂ receptors. To test this, we examined the binding of [³H]raclopride using the same binding paradigm we established for [³H]NMSP, using both sulpiride and raclopride as competitors. Similar to [³H]NMSP binding, MTSET at concentrations of 3 mM or greater inactivated 90% of [³H]raclopride binding in control cells (Q⁻), but only about 50% in quinpirole treated-cells (Q⁺) (data not shown). [³H]Raclopride binding in competition with sulpiride also revealed a two-site binding curve, with a K_{i(s)} = 7.7 ± 2.3 nM for surface D₂ receptors (85.8%) and a K_{i(i)} = 141.8 ± 45.2 μM for intracellular D₂ receptors (14.2%) in control cells (Q⁻). Following quinpirole treatment (Q⁺), 43.1% of D₂ receptors remained on the cell surface (K_{i(s)} = 7.9 ± 3.0 nM) and 56.9% were inside (K_{i(i)} = 120.7 ± 35.8 μM), showing that about 43% of D₂ receptors underwent internalization (Figure 4A).

The similarity between [³H]NMSP and [³H]raclopride binding in competition with sulpiride suggested that [³H]raclopride bound to internal receptors in a manner qualitatively similar to that of [³H]NMSP. In contrast to sulpiride, raclopride competition binding with [³H]NMSP (Figure 4B) showed an overlap of one-site binding curves in control (Q⁻, K_i = 0.26 ± 0.09 nM) and quinpirole treated cells (Q⁺, K_i = 0.28 ± 0.05 nM), confirming that raclopride bound to both surface and internalized D₂ receptors.

Impact of internalization on ligand affinity

The experiments described above demonstrated that most D₂ receptors are at the cell surface under basal conditions whereas about 40% of D₂ receptors are internalized following

quinpirole treatment, and that [^3H]NMSP and [^3H]raclopride bind to both the surface and internalized D_2 receptors. Since MTSET inactivated nearly all binding under control conditions, untreated cells (Q-/MTSET-) could be used to measure binding to surface receptors. Following agonist and MTSET treatments, receptors remaining on the cell surface were inactivated, so treated cells (Q+/MTSET+) could be used to measure binding to internalized receptors. Thus, these two conditions provided independent means to measure the affinity of surface and internalized D_2 receptors with different neuroimaging ligands in saturation and competition studies.

Saturation binding—Under control conditions (Q-/MTSET-), [^3H]NMSP binding showed a K_D value of 0.12 ± 0.02 nM and a B_{max} value of 37.75 pmol/ 10^5 cells (Figure 5A). Saturation binding at internalized receptors (Q+/MSET+) indicated a significant ($p < 0.01$, $n=3$) increase in the [^3H]NMSP K_D (0.48 ± 0.13 nM), suggesting a significant decrease in affinity. As expected, the B_{max} decreased (19.35 pmol/ 10^5 cells) ($p < 0.01$, $n=3$), due to MTSET inactivation of surface receptors following quinpirole treatment, indicating that about 51% of D_2 receptors had undergone internalization. Confirming its accessibility to internalized D_2 receptors, [^3H]raclopride saturation binding also showed a small but significant increase in K_D in quinpirole-treated cells (Q+/MTSET+: $K_D = 1.2 \pm 0.2$ nM, $p < 0.001$, $n=6$) compared to the control cells (Q-/MTSET-: $K_D = 0.5 \pm 0.1$ nM) and a significant reduction in B_{max} (Q-/MTSET-: $B_{\text{max}} = 22.68$ pmol/ 10^5 cells, Q+/MTSET+: $B_{\text{max}} = 8.8$ pmol/ 10^5 cells; Figure 5B), indicating that about 39% of D_2 receptors underwent internalization.

Competition with D_2 antagonists and agonists—Using [^3H]raclopride as the radioligand, competition binding was performed to examine the accessibility of different D_2 antagonist and agonist imaging ligands and control agents to internalized D_2 receptors in treated (Q+/MTSET+) and control cells (Q-/MTSET-). Antagonist competition curve fits are shown in Figure 6, and Figure S1 (in the Supplementary Information), and agonist competition curve fits in Figure S2 (Supplementary Information). As expected, a large decrease in potency to block [^3H]raclopride binding to internalized receptors was observed for sulpiride, indicating the poor accessibility of sulpiride to internalized D_2 receptors (Figure 6A; Table). In contrast, competition with raclopride displayed similar one-site binding curves under both control and internalization/surface D_2R -inactivation conditions (Figure 6B).

Consistent with the saturation binding, raclopride competition also showed significant increases in K_i in MTSET-treated cells following quinpirole (Figure 6B; Table). Similarly, all tested antagonist imaging ligands (Figure S1, Supplementary Information) were able to compete at internalized receptors with high affinity. A small but significant increase in the K_i for quinpirole plus MTSET treated cells was observed in competition with NMSP (Table; Figure S1B), fallypride (Table; Figure S1C), FLB 457 (Table; Figure S1D), and epidepride (Table; Figure S1E). In agonist competition studies, only a modest change in potency to inhibit [^3H]raclopride binding to internalized receptors was observed for the imaging agents, NPA and PHNO (Table; Figure S2A, B), but not the control agent quinpirole (Figure S2C); all were able to compete at internalized receptors with high affinity. In contrast, dopamine

(Table; Figure S2D), which like sulpiride diffuses poorly into cells showed a dramatic reduction in binding to internalized receptors.

For the seven imaging agents, a two-way ANOVA on K_i under the control and internalization/membrane D2R-inactivation conditions (Q-/MTSET- vs. Q+/MTSET+), with ligands as factors revealed a significant effect of condition ($p = 0.003$), ligands ($p < 0.001$) and condition by ligands interactions ($p < 0.001$). Thus, internalization was associated with a small but significant loss of affinity overall. The magnitude of the effect varied among the ligands tested. Post-hoc analysis performed on normalized values revealed that the internalization effect was significantly larger for fallypride and FLB 457, compared to IBZM and NPA, but not significantly different from the other ligands.

DISCUSSION

We examined the impact of D₂ receptor internalization on the binding affinities of D₂ receptor antagonists and agonists commonly used in PET and SPECT imaging studies. Initial experiments in T-REx-293 cells stably transfected with D₂ receptors failed to demonstrate reliable agonist-induced D₂ receptor internalization. Under baseline and following agonist treatment, more than 90% of D₂ receptors remained on the cell surface. In contrast, cells co-transfected with GRK2 and arrestin3 showed robust agonist-induced internalization, confirming that GRK2 and arrestin3 play critical roles in agonist-induced D₂ receptor internalization (Heusler *et al*, 2008; Ito *et al*, 1999; Kim *et al*, 2001; Macey *et al*, 2004; Namkung *et al*, 2009). Quantification of agonist-induced internalization in triple-transfected cells yielded consistent results with four independent methods: flow cytometry (58% internalized fraction), MTSET inactivation (40%), saturation binding (35% with ³H-NMSP; 43% with ³H-raclopride) and sulpiride competition (51% with ³H-NMSP; 39% with ³H-raclopride). Thus, in the triple-transfected cells, agonist treatment caused about 40% of cell surface receptors to undergo internalization.

The ligands [³H]NMSP and [³H]raclopride accessed both surface and internalized receptors. Prior to agonist treatment, membrane-impermeant MTSET abolished the specific binding of both antagonists, indicating that most receptors were indeed on the cell surface. After agonist treatment, the effect of MTSET was lessened, demonstrating specific binding of both ligands to internalized receptors that MTSET could not access. Similarly, sulpiride inhibited most of the binding of both antagonists with high affinity prior to agonist treatment; following agonist treatment, high affinity binding was reduced and low affinity binding increased, presumably reflecting binding of both radiolabeled antagonists to receptors inside the cells. The ability of [³H]NMSP and [³H]raclopride to diffuse into the cells was not unexpected, as [¹¹C]NMSP and [¹¹C]raclopride readily cross the blood brain barrier, which entails diffusion across several cell membranes. Thus, internalized D₂ receptors retain the conformation required for high affinity binding of NMSP and raclopride.

This cellular system provided a straightforward way to compare the affinity of unlabelled ligands for surface and internalized receptors. The affinity measured under basal conditions (Q-/MTSET-) was the affinity at surface receptors, whereas the affinity measured after quinpirole exposure and MTSET inactivation (Q+/MTSET+) was the affinity at internalized

receptors. Comparing [³H]NMSP and [³H]raclopride affinity in saturation studies under Q-/MTSET- and Q+/MTSET+ conditions provided a first indication that affinity of these drugs for internalized receptors was reduced. As the calculation of K_i depends on the K_D , the determination of [³H]raclopride K_D values for surface and internalized receptors was a prerequisite for the competition experiments with the neuroimaging ligands.

[³H]Raclopride competition binding experiments were performed with a number of imaging ligands under both Q-/MTSET- and Q+/MTSET+ conditions. Affinity values measured in this system were consistent with values reported in the literature. The rank order of affinity values was also consistent with values reported in the literature: PHNO, NPA and raclopride < IBZM and fallypride < NMSP < FLB457 and epidepride. Analysis of the competition data revealed a significant effect of receptor internalization on K_i values. Internalization was associated with a small but significant reduction in measured affinity. The magnitude of the affinity change varied amongst ligands, with fallypride and FLB 457 exhibiting larger affinity shifts than IBZM and NPA.

The average decrease in affinity associated with internalization for all the imaging ligands was 2.1 fold. A change of this magnitude would have a direct impact on neuroimaging results. BP is the measured binding parameter and is inversely proportional to K_D ($BP = B_{max}/K_D$). Assuming, for the sake of argument, that all D_2 receptors are on the surface under baseline conditions, and that 50% of receptors are internalized following an amphetamine-induced DA surge, then BP would be reduced by 25%. The magnitude of this decrease is comparable to the BP decrease observed following a amphetamine challenge *in vivo* (Laruelle *et al*, 1997b).

There are several potential caveats that need to be considered in the interpretation of our competition studies. First, incomplete washout of quinpirole could have led to a reduction in the apparent affinity determined in saturation binding analysis after internalization, but the similarity between our saturation and competition results suggest that this is not a confound. Second, the free ligand concentration in the vicinity of internalized receptors might be lower than in the extracellular milieu because of the time required for ligands to traverse the plasma and endosomal membranes to reach internalized receptors. The existence of a gradient between extracellular ligand and endosomal ligand concentrations could give rise to an apparent increase in the K_i measured in the competition experiments. Difficulties in diffusion into cells evidently do translate into changes in apparent affinity, as exemplified by the sulpiride and dopamine experiments. We performed our studies under quasi-equilibrium conditions in an attempt to obviate differences in free ligand concentration across the membrane. Regardless, this should not impact on of the implications for neuroimaging studies in which the extracellular concentration is used as the reference concentration to calculate K_D and BP. Changes in binding affinity revealed here should thus parallel changes in BP observed in neuroimaging studies.

Over expression of arrestin3 could alter the affinity of D_2 receptors for some ligands and a difference between arrestin binding to surface and internal receptors could conceivably contribute to our findings. Indeed arrestin3 binding to purified β_2 -adrenergic receptors substantially increases agonist affinity (> 10-fold) (Gurevich *et al*, 1997). However, we did

not see a consistent effect on the binding of agonists, which should be affected similarly by receptor affinity state: PHNO showed a reduced affinity for internalized receptors while NPA and quinpirole were unaffected. Therefore, it seems unlikely that binding of arrestin3 impacts significantly on binding affinity in our system.

We measured changes in affinity of internalized D₂ receptors 3-4 hrs after triggering internalization and at 4 °C in order to prevent receptors from recycling back to the plasma membrane. It is not known how rapidly or how many D₂ receptors recycle back to the membrane *in vivo*. In HEK-293 at 37 °C, D₂ receptors cells degrade slowly ($t_{1/2} > 7$ h) but recycle rapidly back to the membrane ($t_{1/2} > 30$ min) (Vickery *et al*, 1999). It seems likely that significant numbers of receptors recycle back to the membrane during the course of a neuroimaging experiment. However, this would lessen (rather than magnify) the contribution of internalization to the extent and duration of decreases in BP of radioligands in neuroimaging studies. Finally, it remains possible that the T-REx-293 cells we used do not entirely model the differences in neurons in the receptor microenvironment associated with internalization. This issue will require further studies in neurons.

Constrained by these limitations, the results described in this paper have several implications for the interpretation of D₂ neuroreceptor imaging studies. First, we show that all the tested imaging ligands bind with high but different affinity to surface and internalized receptors. The implication is that the specific binding of ligands observed in PET and SPECT imaging studies is a mixture of binding to surface and internalized receptors. As several of the ligands display different affinities for D₂ receptors based on internalization status, changes in D₂ receptor BP observed in pathological conditions may be due to differences in internalization status. The results generally support the hypothesis that changes in internalization status following interventions that modulate synaptic DA concentrations contribute to changes in observed BP. As addressed in the Introduction, changes in BP persist well beyond acute fluctuations in extracellular DA concentrations, suggesting that mechanisms other than simple binding competition contribute to the sustained BP decrease following a DA surge. Decreased affinity of internalized receptors might be one such mechanism. One way to test this hypothesis would be to correlate the time course of changes in cellular localization of D₂ receptors *in vivo* with the time course of changes in BP following a DA surge.

The differences between ligands in the magnitude of the affinity shift associated with internalization status were not related to differences in affinity, lipophilicity, chemical nature, or pharmacological property (agonists versus antagonists). Furthermore, they were not directly related to the magnitude of changes in *in vivo* binding following manipulation of DA release. Of the eight ligands used in this study, five are unquestionably satisfactory neuroimaging ligands, namely [¹¹C]raclopride, [¹²³I]IBZM, [¹⁸F]fallypride, [¹¹C]NPA and [¹¹C]PHNO. A common property of these imaging ligands is that their moderate affinity and kinetic profile enables proper quantification of D₂ receptor BP in the striatum. The antagonists, [¹¹C]raclopride, [¹²³I]IBZM and [¹⁸F]Fallypride, have been shown to be robustly affected by acute changes in synaptic DA, both in animals and humans. Available evidence suggests that the magnitude of BP decrease after amphetamine is similar for three of these imaging ligands [¹¹C]raclopride, [¹²³I]IBZM and [¹⁸F]fallypride (Cropley *et al*,

2008; Laruelle, 2000; Mukherjee *et al*, 2005; Narendran *et al*, 2009; Riccardi *et al*, 2006; Slifstein *et al*, 2004). The differences in affinity shifts amongst the three ligands induced by internalization (fallypride>raclopride>IBZM) observed here suggest that the affinity shift is not the only factor contributing to the long lasting BP changes observed in neuroimaging experiments. Changes that would affect the B_{max} in the brain without changing the affinity, such as receptor modification or degradation, might not be captured by the present results. Further work will be needed to test these putative factors.

The vulnerability of [^{11}C]NPA to changes in endogenous DA is larger than that of [^{11}C]raclopride, an observation that has been attributed to fact that [^{11}C]NPA, being a full agonist, binds preferentially to D_2 receptors in the high affinity state, a population of receptors expected to be more affected by changes in synaptic DA (Narendran *et al*, 2004). The difference in affinity shift induced by internalization between these ligands (raclopride>NPA) seen in the present studies does not jive with the magnitude of BP decrease ([^{11}C]NPA>[^{11}C]raclopride) after amphetamine (Narendran *et al*, 2004). The *in vivo* vulnerability of [^{11}C]PHNO to DA changes is even higher than that of [^{11}C]NPA, because [^{11}C]PHNO displays higher affinity for D_3 compared to D_2 receptors and D_3 receptors have higher affinity for DA than D_2 receptors (Graff-Guerrero *et al*, 2009; Narendran *et al*, 2006; Rabiner *et al*, 2009). In regions such as the dorsal striatum where D_2 receptors are responsible for most of the [^{11}C]PHNO and [^{11}C]NPA binding signals (Searle *et al*), changes in [^{11}C]PHNO BP induced by amphetamine are of the same magnitude as [^{11}C]NPA (Narendran *et al*, 2006; Rabiner *et al*, 2009). In the experiments reported here, the affinity shift of PHNO was numerically larger than for NPA, an observation inconsistent with internalization alone accounting for the results of the imaging studies.

Interpreting the results for the very high affinity antagonists [^{11}C]NMSP, [^{11}C]FLB457 and [^{123}I]epidepride is more complex. Proper *in vivo* quantification of D_2 receptors BP with these ligands in high D_2 receptor density regions such as the striatum is practically impossible due to the protracted time required for these ligands to reach equilibrium and the vulnerability of their uptake to changes in blood flow. Many contradictory studies have thus been reported in the literature; studies with [^{11}C]NMSP or analogues reported increased, decreased or no change in BP following amphetamine (Bischoff and Gunst, 1997; Bischoff *et al*, 1991; Hartvig *et al*, 1997; Leslie and Bennett Jr., 1987). Two studies with [^{123}I]epidepride suggested no changes in BP following amphetamine (Al-Tikriti *et al*, 1994; Tibbo *et al*, 1997). From a kinetic point of view, [^{11}C]FLB457 is adequate to measure D_2 receptor BP in cortical regions, where the concentration of D_2 receptors is much lower. Consistent with this, we have found in humans that the BP of [^{11}C]FLB457 is reduced in the cortex following amphetamine (Narendran *et al*, 2009); however, such a change was not found by others (Aalto *et al*, 2009; Okauchi *et al*, 2001). The low signal-to-noise associated with measurement of cortical D_2 receptors might explain this discrepancy. Because of the uncertain nature and magnitude of the vulnerability of these ligands to endogenous DA in imaging paradigms, only a limited comparison with the present results is possible.

In conclusion, we have developed an *in vitro* system suitable for independent measurements of the affinity of ligands to surface and internalized D_2 receptors. Testing of eight commonly used D_2 receptor neuroimaging ligands showed that all ligands bind with high affinity to

both surface and internalized receptors. Receptor internalization is associated with a small but significant reduction in binding affinity for six of the eight ligands. To the extent that these findings can be extrapolated to the *in vivo* condition, our results suggest that D₂ receptor trafficking may affect the signal measured in neuroimaging studies and may play a role in the sequence of events leading to changes in D₂ receptor BP following subsequent to fluctuations in synaptic DA concentrations. However, differences in affinity shifts among the ligands suggest that factors other than receptor trafficking are likely to be involved in these long lasting changes. Further work will be needed to determine the role of receptor trafficking in these responses, as well as to identify and validate other mechanisms.

Supplementary Material

Refer to Web version on PubMed Central for supplementary material.

ACKNOWLEDGEMENTS

We thank Brian K. Clinton and Todd J. Harris for initial experiments. This work was supported by the NIMH Conte Center on the *Neurobiology of Dopamine in Schizophrenia* MH066171 (ML, SR), NIH grants DA022413 and MH54137 (JAJ), DA000356 (SR), NARSAD (NG), by GlaxoSmithKline, and by the Lieber Center for Schizophrenia Research and Treatment at Columbia University.

REFERENCES

- Aalto S, Hirvonen J, Kaasinen V, Hagelberg N, Kajander J, Nagren K, et al. The effects of d-amphetamine on extrastriatal dopamine D₂/D₃ receptors: a randomized, double-blind, placebo-controlled PET study with [11C]FLB 457 in healthy subjects. *Eur J Nucl Med Mol Imaging*. 2009; 36(3):475–483. [PubMed: 18985345]
- Abi-Dargham A, Rodenhiser J, Printz D, Zea-Ponce Y, Gil R, Kegeles LS, et al. Increased baseline occupancy of D₂ receptors by dopamine in schizophrenia. *Proc Natl Acad Sci U S A*. 2000; 97(14): 8104–8109. [PubMed: 10884434]
- Al-Tikriti MS, Baldwin RB, Zea-Ponce Y, Sybriska E, Zoghbi S, Laruelle M, et al. Comparison of three high affinity SPECT radiotracers for the dopamine D₂ receptors. *Nucl Med Biol*. 1994; 21:179–188. [PubMed: 9234281]
- Bischoff S, Gunst F. Distinct binding patterns of [³H]raclopride and [³H]spiperone at dopamine D₂ receptors in vivo in rat brain. Implications for PET studies. *J Recept Signal Transduct Res*. 1997; 17(1-3):419–431. [PubMed: 9029505]
- Bischoff S, Krauss J, Grunenwald C, Gunst F, Heinrich M, Schaub M, et al. Endogenous dopamine (DA) modulates [³H]spiperone binding in vivo in rat brain. *J Recept Res*. 1991; 11:163–175. [PubMed: 1886078]
- Breier A, Su TP, Saunders R, Carson RE, Kolachana BS, de Bartolomeis A, et al. Schizophrenia is associated with elevated amphetamine-induced synaptic dopamine concentrations: evidence from a novel positron emission tomography method. *Proc Natl Acad Sci U S A*. 1997; 94(6):2569–2574. [PubMed: 9122236]
- Carson, RE.; Channing, MA.; Vuong, B.; Watabe, H.; Herscovitch, P.; Eckelman, WC. Amphetamine-induced dopamine release: Duration of action assessed with [11C]raclopride in anesthetized monkeys.. In: Gjedde, A., editor. *Physiological Imaging of the Brain with PET*. Academic Press; San Diego: 2001. p. 205-209.
- Cropley V, Innis R, Nathan P, Brown A, Sangare J, Lerner A, et al. Small effect of dopamine release and no effect of dopamine depletion on [18F]fallypride binding in healthy humans. *Synapse*. 2008; 62(6):399–408. [PubMed: 18361438]
- de Paulis T, Janowsky A, Kessler RM, Clanton JA, Smith HE. (S)-N-[(1-ethyl-2-pyrrolidinyl)methyl]-5-[125I]iodo-2-methoxybenzamide hydrochloride, a new selective radioligand for dopamine D-2 receptors. *J Med Chem*. 1988; 31(10):2027–2033. [PubMed: 3172140]

- Ginovart N, Galineau L, Willeit M, Mizrahi R, Bloomfield PM, Seeman P, et al. Binding characteristics and sensitivity to endogenous dopamine of [¹¹C]-(+)-PHNO, a new agonist radiotracer for imaging the high-affinity state of D2 receptors in vivo using positron emission tomography. *J Neurochem.* 2006; 97(4):1089–1103. [PubMed: 16606355]
- Goggi JL, Sardini A, Egerton A, Strange PG, Grasby PM. Agonist-dependent internalization of D2 receptors: Imaging quantification by confocal microscopy. *Synapse.* 2007; 61(4):231–241. [PubMed: 17230553]
- Graff-Guerrero A, Redden L, Abi-Saab W, Katz DA, Houle S, Barsoum P, et al. Blockade of [¹¹C]-(+)-PHNO binding in human subjects by the dopamine D3 receptor antagonist ABT-925. *Int J Neuropsychopharmacol.* 2009:1–15.
- Gurevich VV, Pals-Rylaarsdam R, Benovic JL, Hosey MM, Onorato JJ. Agonist-receptor-arrestin, an alternative ternary complex with high agonist affinity. *J Biol Chem.* 1997; 272(46):28849–28852. [PubMed: 9360951]
- Hartvig P, Torstenson R, Tedroff J, Watanabe Y, Fasth KJ, Bjurling P, et al. Amphetamine effects on dopamine release and synthesis rate studied in the Rhesus monkey brain by positron emission tomography. *J Neural Transm.* 1997; 104(4-5):329–339. [PubMed: 9295169]
- Heusler P, Newmantancredi A, Loock T, Cussac D. Antipsychotics differ in their ability to internalise human dopamine D2S and human serotonin 5-HT1A receptors in HEK293 cells. *Eur J Pharmacol.* 2008; 581(1-2):37–46. [PubMed: 18190908]
- Honda F, Satoh Y, Shimomura K, Satoh H, Noguchi H, Uchida S, et al. Dopamine receptor blocking activity of sulpiride in the central nervous system. *Jpn J Pharmacol.* 1977; 27(3):397–411. [PubMed: 562433]
- Ichikawa J, Meltzer HY. The effect of chronic atypical antipsychotic drugs and haloperidol on amphetamine-induced dopamine release in vivo. *Brain Res.* 1992; 574(1-2):98–104. [PubMed: 1379112]
- Ito K, Haga T, Lamah J, Sadee W. Sequestration of dopamine D2 receptors depends on coexpression of G-protein-coupled receptor kinases 2 or 5. *Eur J Biochem.* 1999; 260(1):112–119. [PubMed: 10091590]
- Javitch JA, Li X, Kaback J, Karlin A. A cysteine residue in the third membrane-spanning segment of the human D2 dopamine receptor is exposed in the binding-site crevice. *Proc Natl Acad Sci U S A.* 1994; 91(22):10355–10359. [PubMed: 7937955]
- Javitch JA, Shi L, Simpson MM, Chen J, Chiappa V, Visiers I, et al. The fourth transmembrane segment of the dopamine D2 receptor: accessibility in the binding-site crevice and position in the transmembrane bundle. *Biochemistry.* 2000; 39(40):12190–12199. [PubMed: 11015197]
- Kegeles LS, Abi-Dargham A, Zea-Ponce Y, Rodenhiser-Hill J, Mann JJ, Van Heertum RL, et al. Modulation of amphetamine-induced striatal dopamine release by ketamine in humans: implications for schizophrenia. *Biol Psychiatry.* 2000; 48(7):627–640. [PubMed: 11032974]
- Kessler RM, Ansari MS, de Paulis T, Schmidt DE, Clanton JA, Smith HE, et al. High affinity dopamine D₂ receptor radioligands. 1. Regional rat brain distribution of iodinated benzamides. *J Nucl Med.* 1991; 32:1593–1600. [PubMed: 1831229]
- Kim KM, Valenzano KJ, Robinson SR, Yao WD, Barak LS, Caron MG. Differential regulation of the dopamine D2 and D3 receptors by G protein-coupled receptor kinases and β-arrestins. *J Biol Chem.* 2001; 276(40):37409–37414. [PubMed: 11473130]
- Laruelle M. Imaging neurotransmission with *in vivo* binding competition techniques: a critical review. *J Cereb Blood Flow Metab.* 2000; 20(3):423–451. [PubMed: 10724107]
- Laruelle M, Abi-Dargham A, van Dyck C, Gil R, De Souza C, Erdos J, et al. Single photon emission computerized tomography imaging of amphetamine-induced dopamine release in drug free schizophrenic subjects. *Proc Natl Acad Sci USA.* 1996; 93:9235–9240. [PubMed: 8799184]
- Laruelle M, D'Souza CD, Baldwin RM, Abi-Dargham A, Kanes SJ, Fingado CL, et al. Imaging D2 receptor occupancy by endogenous dopamine in humans. *Neuropsychopharmacology.* 1997a; 17(3):162–174. [PubMed: 9272483]
- Laruelle M, Iyer RN, al-Tikriti MS, Zea-Ponce Y, Malison R, Zoghbi SS, et al. Microdialysis and SPECT measurements of amphetamine-induced dopamine release in nonhuman primates. *Synapse.* 1997b; 25(1):1–14. [PubMed: 8987142]

- Leslie CA, Bennett JP Jr. Striatal D1- and D2-dopamine receptor sites are separately detectable in vivo. *Brain Res.* 1987; 415:90–97. [PubMed: 2957025]
- Loc'h C, Halldin C, Bottlaender M, Swahn CG, Moresco RM, Maziere M, et al. Preparation of [76Br]FLB 457 and [76Br]FLB 463 for examination of striatal and extrastriatal dopamine D-2 receptors with PET. *Nucl Med Biol.* 1996; 23(6):813–819. [PubMed: 8940725]
- Macey TA, Gurevich VV, Neve KA. Preferential Interaction between the dopamine D2 receptor and Arrestin2 in neostriatal neurons. *Mol Pharmacol.* 2004; 66(6):1635–1642. [PubMed: 15361545]
- Martinez D, Narendran R, Foltin RW, Slifstein M, Hwang DR, Broft A, et al. Amphetamine-induced dopamine release: markedly blunted in cocaine dependence and predictive of the choice to self-administer cocaine. *Am J Psychiatry.* 2007; 164(4):622–629. [PubMed: 17403976]
- Mizuchi A, Kitagawa N, Miyachi Y. Regional distribution of sultopride and sulpiride in rat brain measured by radioimmunoassay. *Psychopharmacology (Berl).* 1983; 81(3):195–198. [PubMed: 6417707]
- Mukherjee J, Christian BT, Narayanan TK, Shi B, Collins D. Measurement of d-amphetamine-induced effects on the binding of dopamine D-2/D-3 receptor radioligand, 18F-fallypride in extrastriatal brain regions in non-human primates using PET. *Brain Res.* 2005; 1032(1-2):77–84. [PubMed: 15680944]
- Namkung Y, Dipace C, Javitch JA, Sibley DR. G protein-coupled receptor kinase-mediated phosphorylation regulates post-endocytic trafficking of the D2 dopamine receptor. *J Biol Chem.* 2009; 284(22):15038–15051. [PubMed: 19332542]
- Narendran R, Frankle WG, Mason NS, Rabiner EA, Gunn RN, Searle GE, et al. Positron emission tomography imaging of amphetamine-induced dopamine release in the human cortex: a comparative evaluation of the high affinity dopamine D2/3 radiotracers [11C]FLB 457 and [11C]fallypride. *Synapse.* 2009; 63(6):447–461. [PubMed: 19217025]
- Narendran R, Hwang DR, Slifstein M, Talbot PS, Erritzoe D, Huang Y, et al. In vivo vulnerability to competition by endogenous dopamine: comparison of the D2 receptor agonist radiotracer (-)-N-[11C]propyl-norapomorphine ([11C]NPA) with the D2 receptor antagonist radiotracer [11C]-raclopride. *Synapse.* 2004; 52(3):188–208. [PubMed: 15065219]
- Narendran R, Slifstein M, Guillin O, Hwang Y, Hwang DR, Scher E, et al. Dopamine (D(2/3)) receptor agonist positron emission tomography radiotracer [(11)C]-(+)-PHNO is a D(3) receptor preferring agonist in vivo. *Synapse.* 2006; 60(7):485–495. [PubMed: 16952157]
- Narendran R, Slifstein M, Hwang DR, Hwang Y, Scher E, Reeder S, et al. Amphetamine-induced dopamine release: duration of action as assessed with the D2/3 receptor agonist radiotracer (-)-N-[11C]propyl-norapomorphine ([11C]NPA) in an anesthetized nonhuman primate. *Synapse.* 2007; 61(2):106–109. [PubMed: 17117423]
- Okauchi T, Suhara T, Maeda J, Kawabe K, Obayashi S, Suzuki K. Effect of endogenous dopamine on endogenous dopamine on extrastriated [11C]FLB 457 binding measured by PET. *Synapse.* 2001; 41(2):87–95. [PubMed: 11400175]
- Paspalas CD, Rakic P, Goldman-Rakic PS. Internalization of D2 dopamine receptors is clathrin-dependent and select to dendro-axonic appositions in primate prefrontal cortex. *Eur J Neurosci.* 2006; 24(5):1395–1403. [PubMed: 16987224]
- Perry SJ, Lefkowitz RJ. Arresting developments in heptahelical receptor signaling and regulation. *Trends Cell Biol.* 2002; 12(3):130–138. [PubMed: 11859025]
- Rabiner EA, Slifstein M, Nobrega J, Plisson C, Huiban M, Raymond R, et al. In vivo quantification of regional dopamine-D3 receptor binding potential of (+)-PHNO: Studies in non-human primates and transgenic mice. *Synapse.* 2009; 63(9):782–793. [PubMed: 19489048]
- Rees S, Coote J, Stables J, Goodson S, Harris S, Lee MG. Bicistronic vector for the creation of stable mammalian cell lines that predisposes all antibiotic-resistant cells to express recombinant protein. *Biotechniques.* 1996; 20(1):102–110. [PubMed: 8770413]
- Riccardi P, Li R, Ansari MS, Zald D, Park S, Dawant B, et al. Amphetamine-induced displacement of [18F] fallypride in striatum and extrastriatal regions in humans. *Neuropsychopharmacology.* 2006; 31(5):1016–1026. [PubMed: 16237395]

- Searle G, Beaver JD, Comley RA, Bani M, Tziortzi A, Slifstein M, et al. Imaging dopamine D3 receptors in the human brain with Positron Emission Tomography, [¹¹C]PHNO, and a selective D3 receptor antagonist. *Biol Psychiatry*. in submission.
- Slifstein M, Narendran R, Hwang DR, Sudo Y, Talbot PS, Huang Y, et al. Effect of amphetamine on [¹⁸F]fallypride in vivo binding to D₂ receptors in striatal and extrastriatal regions of the primate brain: Single bolus and bolus plus constant infusion studies. *Synapse*. 2004; 54(1):46–63. [PubMed: 15300884]
- Tibbo P, Silverstone PH, McEwan AJ, Scott J, Joshua A, Golberg K. A single photon emission computed tomography scan study of striatal dopamine D2 receptor binding with 123I-epidepride in patients with schizophrenia and controls. *J Psychiatry Neurosci*. 1997; 22(1):39–45. [PubMed: 9002391]
- Tsao P, Cao T, von Zastrow M. Role of endocytosis in mediating downregulation of G-protein-coupled receptors. *Trends Pharmacol Sci*. 2001; 22(2):91–96. [PubMed: 11166853]
- van Berckel BN, Kegeles LS, Waterhouse R, Guo N, Hwang DR, Huang Y, et al. Modulation of amphetamine-induced dopamine release by group II metabotropic glutamate receptor agonist LY354740 in non-human primates studied with positron emission tomography. *Neuropsychopharmacology*. 2006; 31(5):967–977. [PubMed: 16177807]
- Vickery RG, von Zastrow M. Distinct dynamin-dependent and -independent mechanisms target structurally homologous dopamine receptors to different endocytic membranes. *J Cell Biol*. 1999; 144(1):31–43. [PubMed: 9885242]
- Volkow ND, Fowler JS, Logan J, Alexoff D, Zhu W, Telang F, et al. Effects of modafinil on dopamine and dopamine transporters in the male human brain: clinical implications. *JAMA*. 2009; 301(11): 1148–1154. [PubMed: 19293415]
- Volkow ND, Wang GJ, Fowler JS, Logan J, Gatley SJ, Hitzemann R, et al. Decreased striatal dopaminergic responsiveness in detoxified cocaine-dependent subjects. *Nature*. 1997; 386(6627): 830–833. [PubMed: 9126741]
- Wilson AA, McCormick P, Kapur S, Willeit M, Garcia A, Hussey D, et al. Radiosynthesis and evaluation of [¹¹C]-(+)-4-propyl-3,4,4a,5,6,10b-hexahydro-2H-naphtho[1,2-b][1,4]oxazin-9-ol as a potential radiotracer for in vivo imaging of the dopamine D2 high-affinity state with positron emission tomography. *J Med Chem*. 2005; 48(12):4153–4160. [PubMed: 15943487]

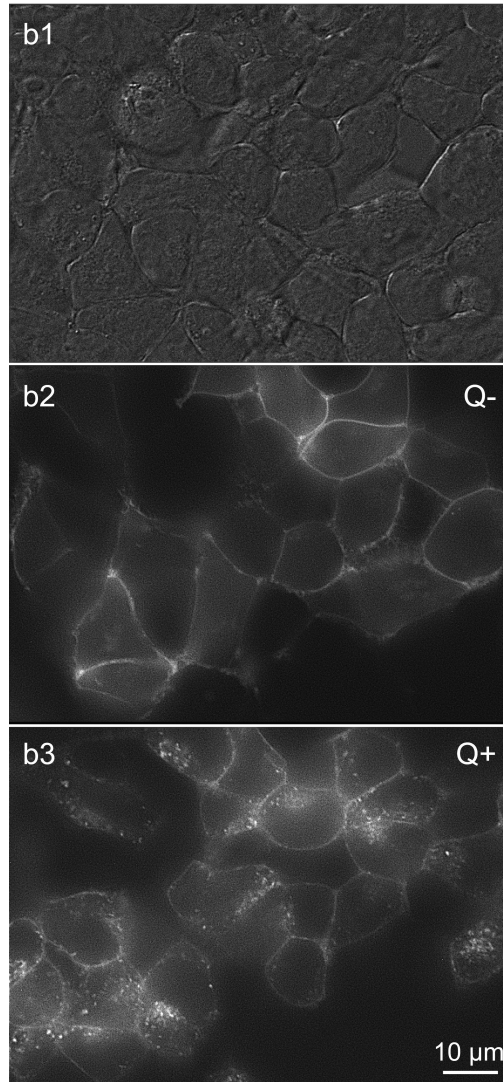
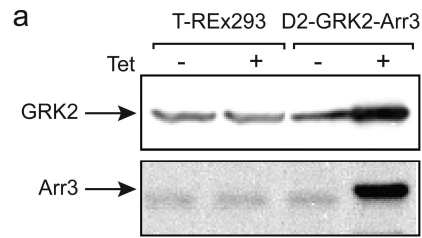


Figure 1. Visualization of GRK2 and arrestin3 enhanced quinpirole-induced D₂ receptor internalization

T-REx-293 cells were triple transfected with D₂ receptors, with the FLAG epitope on the extracellular N-terminus and yellow-fluorescent protein (YFP) on the intracellular C-terminus of D₂ receptors, GRK2 and arrestin3 (Arr3). **a.** Immunoblot analysis of preparations from T-REx-293 control and D₂-GRK2-Arr3 triple-transfected cells. Tetracycline had no effect on basal expression of GRK2 and arrestin3 in control T-REx-293 cells (left), while it induced robust expression of GRK2 and arrestin3 in the triple-transfected cells. GRK2 and arrestin3 proteins were detected by polyclonal anti-GRK2 and

anti-arrestin3 antibodies, respectively. **b.** Cells were treated with tetracycline and then viewed under DIC optics (**b1**) or epic-fluorescence (**b2**), and then again following quinpirole treatment (**b3**). Under control condition (Q-), D₂ receptors were mainly expressed at the cell surface, as indicated by the surface fluorescence labeling of Zenon anti-FLAG and D₂ receptor-YFP fluorescence (**b2**). Quinpirole (Q+) induced a dramatic redistribution of EYFP fluorescence into a punctate intracellular pattern, reflecting robust D₂ receptor internalization (**b3**). Cells have shifted shape and position during the quinpirole incubation so the images are not directly super imposable.

Author Manuscript

Author Manuscript

Author Manuscript

Author Manuscript

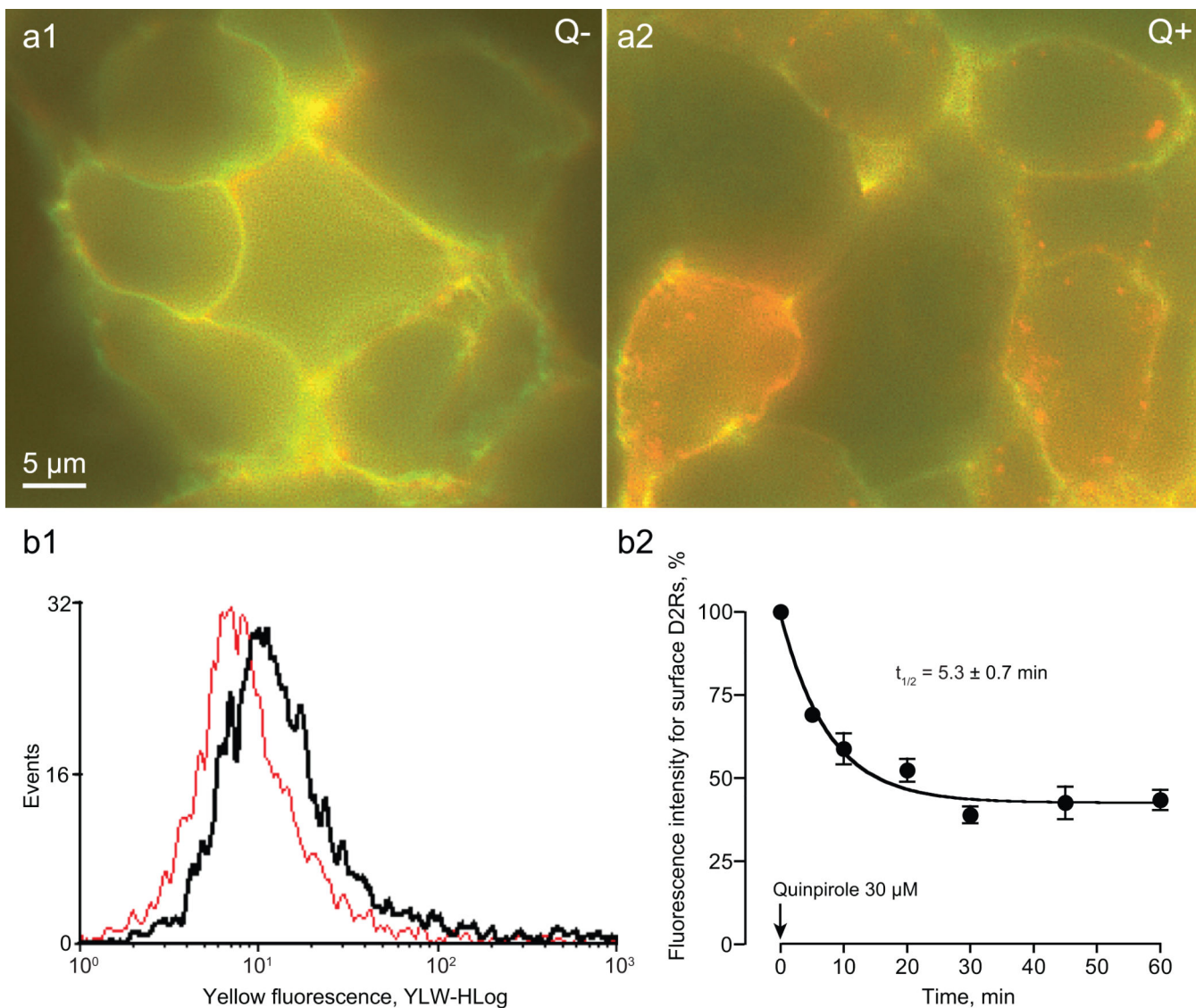


Figure 2. Fluorescence imaging and quantification of quinpirole-induced D₂ receptor internalization

A1. Surface D₂ receptors were visualized with Zenon anti-FLAG Fab fragments directed to the FLAG epitope on the extracellular N-terminus (digitized to green) and the EYFP fluorescence of the EYFP tag on the D₂ receptor C-terminus (digitized to red) in control cells (Q⁻). The overlap in the labeling appears yellow in the color merge shown. **A2.** Following quinpirole treatment (Q⁺), internalized D₂ receptors show solely EYFP fluorescence (red). **B.** Quinpirole-induced D₂ receptor internalization was quantitated using flow cytometry. **B1.** The histogram shows the distribution of fluorescence intensity for surface D₂ receptors before (black) and after (red) quinpirole treatment. **B2.** Time course studies (n = 3; time constant as indicated) revealed that after quinpirole treatment, 42% D₂ receptors remained on the surface, implying that ~58% underwent internalization.

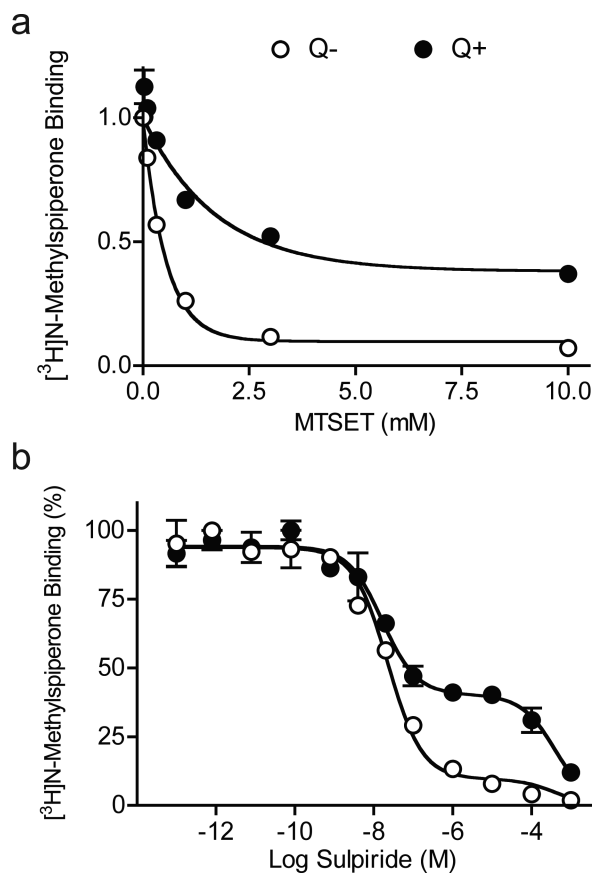


Figure 3. Effect of MTSET and competition with sulpiride on [³H]NMSP binding
 Binding assays were performed in intact cells using [³H]NMSP and quinpirole to induce internalization. **A.** Surface receptors were inactivated with increasing concentrations of MTSET. Under control conditions (○, Q⁻), MTSET inactivated 90% of [³H]NMSP binding. After quinpirole treatment (●, Q⁺), MTSET inactivated only 55% of [³H]NMSP binding, indicated that ~45% of D₂ receptor underwent internalization. **B.** Surface receptors were blocked with the relatively membrane-impermeant antagonist sulpiride. Under control conditions (○, Q⁻), sulpiride competition binding showed a two-site [³H]NMSP binding curve; the majority of D₂ receptors (90%) were accessible to sulpiride and so subject to competition at high affinity ($K_{i(s)} = 9.1 \pm 1.0$ nM), while only a small minority (10%), presumably internalized, were relatively inaccessible and so subject to competition at low affinity ($K_{i(i)} = 142.5 \pm 26.8$ μM). Following quinpirole treatment (●, Q⁺), the high affinity [³H]NMSP binding was reduced to 55%, while the low affinity binding increased to 45%, consistent with robust D₂ receptor internalization.

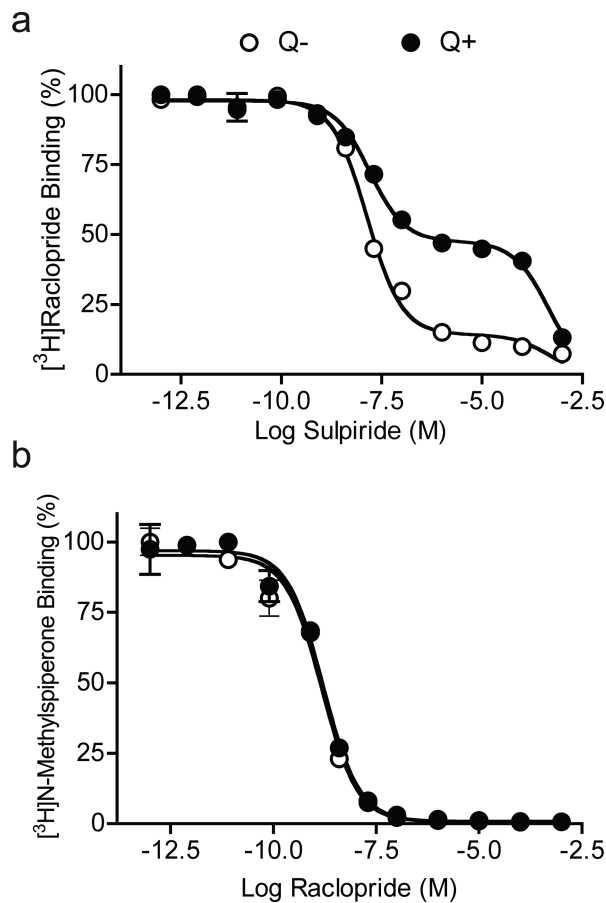


Figure 4. Competition binding of $[^3\text{H}]\text{raclopride}$ or $[^3\text{H}]\text{NMSP}$ under control and internalization conditions

A. $[^3\text{H}]\text{Raclopride}$ binding in competition with sulpiride. A two-site binding curve was observed in control cells (○, Q-). Most D_2 receptors (85.8%) were on the surface and showed high-affinity ($\text{K}_{\text{i}(\text{s})} = 7.7 \pm 2.3 \text{ nM}$). A small proportion (14.2%) were internalized and showed low affinity binding ($\text{K}_{\text{i}(\text{i})} = 141.8 \pm 45.2 \mu\text{M}$). Following quinpirole treatment (●, Q+), 43.1% of D_2 receptors remained on the surface ($\text{K}_{\text{i}(\text{s})} = 7.9 \pm 3.0 \text{ nM}$) and 56.9% were internalized ($\text{K}_{\text{i}(\text{i})} = 120.7 \pm 35.8 \mu\text{M}$). **B.** $[^3\text{H}]\text{NMSP}$ binding in competition with raclopride. Competition experiments showed indistinguishable one-site binding curves between control (○, Q-; $\text{K}_{\text{i}} = 0.26 \pm 0.09 \text{ nM}$) and quinpirole treated cells (●, Q+; $\text{K}_{\text{i}} = 0.28 \pm 0.05 \text{ nM}$). Thus, like NMSP, raclopride readily accesses internalized D_2 receptors.

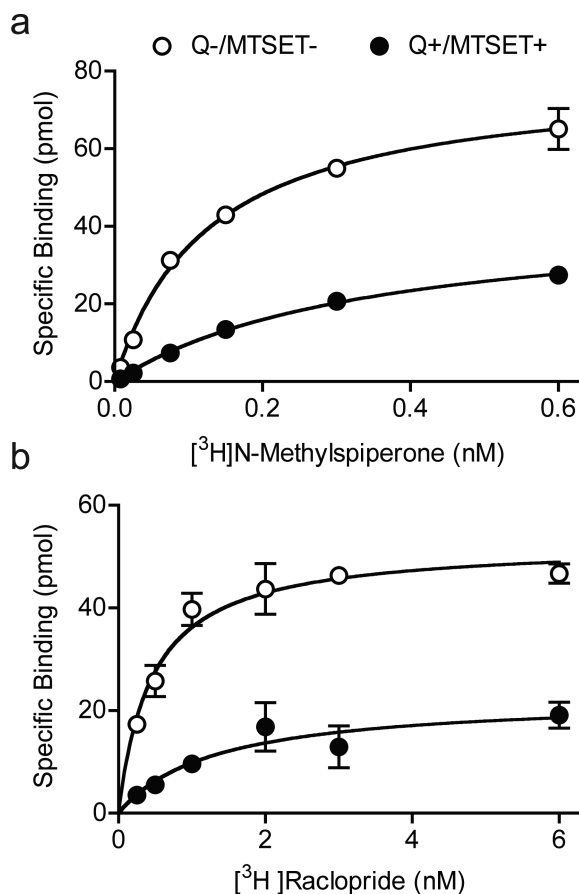


Figure 5. Saturation binding to surface and internalized D₂ receptors

A. Under control conditions, when most receptors are on the surface, [³H]NMSP saturation binding showed a one-site binding curve with a K_D of 0.12 ± 0.02 nM (○, Q-/MTSET-). Following quinpirole and inactivation of surface receptors with MTSET, the remaining functional internalized D₂ receptors showed a one-site binding curve with a lower affinity K_D of 0.48 ± 0.13 nM (●, Q+/MTSET+). Based on the reduction in the B_{max} , ~50% of D₂ receptors underwent internalization. **B.** Under control conditions, [³H]Raclopride saturation binding showed a K_D of 0.5 ± 0.1 nM. Following quinpirole and MTSET, binding showed a lower affinity K_D of 1.2 ± 0.2 nM. Based on the reduction in the B_{max} with Raclopride binding, ~40% of D₂ receptors underwent internalization.

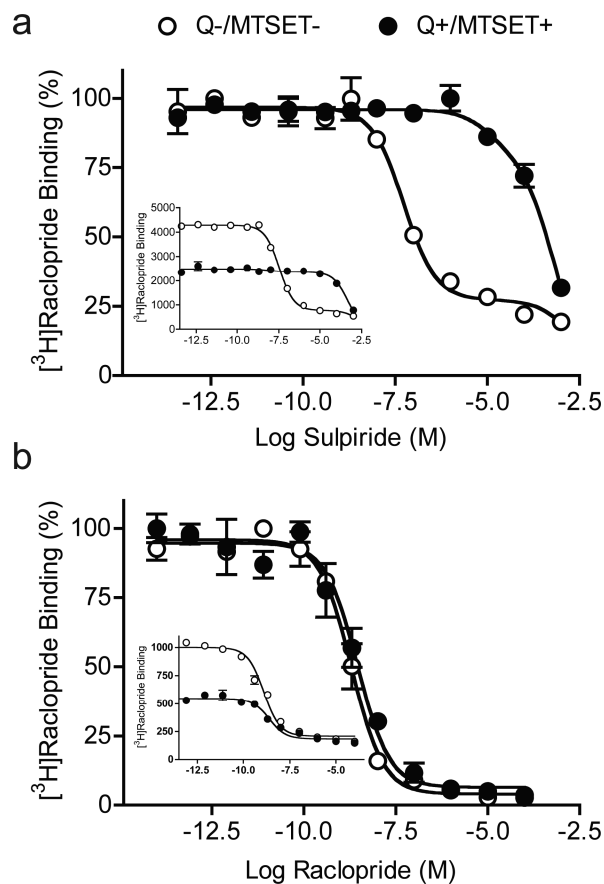


Figure 6. Sulpiride and raclopride competition binding with [³H]raclopride in MTSET-treated cells

A. Competition with sulpiride displayed two different binding curves under control and internalization conditions. A two-site [³H]raclopride binding curve showed that the majority (80.9%) of D₂ receptors were on the surface ($K_{i(s)} = 10.3 \pm 12.3$ nM) in control (○, Q-/MTSET-), and a one-site binding curve indicated the poor accessibility ($K_{i(i)} = 206.0 \pm 23.6$ μM) of sulpiride to internalized D₂ receptors in treated cells (●, Q+/MTSET+). **B.** In contrast, raclopride competition binding displayed similar one-site binding curves under both control and internalization conditions, with about 2-fold increases in the K_i as indicated by the right-shift of the binding curve in treated cells (●) compared to control (○). The insets in **A** and **B** show the same binding data as in **A** and **B**, respectively, but without normalizing the binding parameters to allow for quantitative comparison of binding to control and treated cells.

Table

Effect of internalization on the affinity of commonly used neuroimaging agents

Type of ligand	Pharmacology	Ligand (number of experiments)	Surface D2 receptor (Q-/MTSET-) $K_{i(0)}$, nM	Internalized D2 receptor (Q+/MTSET+) $K_{i(0)}$, nM	Affinity shift $K_{i(0)}/K_{i(s)}$	Lipophilicity (Log $P_{i(0)}$ or Log $kw_{i(0)}$)
Imaging	Antagonist	Raclopride (6)	0.50 ± 0.08	1.00 ± 0.35*	2.1	1.3 ^a †
		FLB 457 (5)	0.03 ± 0.01	0.09 ± 0.02**	3.0	1.9 ^b †
		Epidopride (6)	0.01 ± 0.01	0.03 ± 0.01*	2.4	2.1 ^c †
		Fallypride (6)	0.32 ± 0.06	0.92 ± 0.31**	2.9	2.4 ^a †
		IBZM (9)	0.19 ± 0.05	0.23 ± 0.11	1.2	2.8 ^a †
		NMSP (6)	0.07 ± 0.01	0.13 ± 0.02**	1.9	3.3 ^a †
		PHNO (9)	2.62 ± 0.56	5.67 ± 2.90*	2.2	2.1 ^d †
		NPA (6)	0.97 ± 0.28	1.02 ± 0.33	1.1	2.5 ^d †
		Control	Agonist	Dopamine (6)	870.3 ± 146	19,337 ± 4265**
Quinpirole (7)	900.4 ± 138.3			856.1 ± 120.5	1.0	2.4 [#] †
Sulpiride (3)	10.3 ± 2.3			202,000 ± 25,300**	19,600	1.3 ^e †

K_i values were measured for surface (K_{i(s)}), Q-/MTSET- conditions) and internalized (K_{i(i)}) Q+/MTSET+ conditions) D2 receptors.

* $p < 0.01$ vs K_{i(s)}

** $p < 0.001$ vs. K_{i(s)}, *t*-Test. Two-way ANOVA restricted to the imaging agents with conditions (Q-/MTSET- versus Q+/MTSET+) and ligands as factors further revealed a significant effect of conditions ($p = 0.003$), ligands ($p < 0.001$) and condition by ligands interactions ($p < 0.001$).

Calculated with Chemdraw Ultra 11.0.1 (CambridgeSoft, Cambridge, MA).

^a Laruelle, 2000

^b Loch et al., 1996

^c Kessler et al., 1991

^d Wilson et al., 2005

^e de Paulis et al., 1988